Chapter 1

Optics on chip

It is unecessary to emphasize the importance of electronics integrated circuits to the current world. But it is worth to investigate if it is possible to create the same structure in different fields. In this investigation one can notice the two crucial feature of the success. The use of massivelly parallel device patterning enabled by photolitography and the search to decrease device size to its physical limits.

Three ramification using the microfabrication process have come of age in the last decade: Microfluidics, micro-mechanical devices (MEMs) and integrated optics. Microfluidics enables the possibility of massive chemical analysis which revolutionized genetic research, enabling operation such as DNA sequencing to be performed at a fraction of time that was done before[citation]. Micromechanical devices [weinstein thesis]. Integrated optics which has the potential of large bandwidth data transfer and spectroscopic analysis, and possibly quantum processing.

we chose integrated optics ....

1.1 Broad picture

The basic feature ones needs

The platform in which optic on chip works consists in the use of a high index of refraction material surrounded by a material with lower index of refraction to guide light in the higher refrative index material using the total internal reflection. We call a slab waveguide when a higher refractive index medium is cladded by a lower index medium in only dimension. Light that is guided in the higher index material can be treated a two dimensional wave. In this regime, knowledge of free space optics can be applied to design devices. Components like, lenses, mirrors, concave mirrors, prisms, gratings can be readliy visualized[citations][pictures].

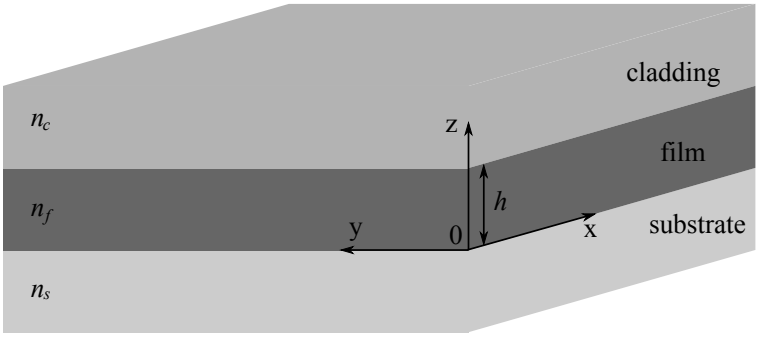

Figure 1.2.1:

Another component is wire waveguide, where a high index of refraction material is surrounded by lower index material in two dimension. This structure transport light like electrons on copper wire. This structure is widely used as fiber optics, where system built on fiber optics can implemented on chip waveguides.

In chapter we are going to dicuss the physical principles necessary to design components in integrated optics.

1.2 Slab waveguide

We define a slab waveguide as a system comprised of an infinite film (which will be also referred as core) of thicknes h and index of refraction n_f over a substrate with index of refraction $n_s$and cladded by a material whose index of refraction is n_c. As stated earlyer the index of refraction in the guiding film needs to be greater than its surroundings, this condition is stated in the relation:

$$n_f > n_s \geqslant n_c \tag{1.2.1}$$

where we left the inequality $n_s \geqslant n_c$ for sake of generallity and we take the higher index of refraction index to be the substrate.

The Maxwell equation in frequency domain for given system is:

$$\begin{aligned} \nabla \cdot \epsilon_0 \epsilon(z)\, \mathbf{E}(\mathbf{r},\omega) &= 0 && (1.2.2)\\ \nabla \times \mathbf{E}(\mathbf{r},\omega) &= i\omega\mu_0 \mathbf{H}(\mathbf{r},\omega) && (1.2.3)\\ \nabla \cdot \mu_0 \mathbf{H}(\mathbf{r},\omega) &= 0 && (1.2.4)\\ \nabla \times \mathbf{H}(\mathbf{r},\omega) &= -i\omega\epsilon_0 \epsilon(z)\, \mathbf{E}(\mathbf{r},\omega) && (1.2.5) \end{aligned}$$

where the net charge charge and current density was considered zero, and the permeability of the materials was considered to be μ_0. The relative dielectric constant in accordance with begining of the section is:

$$\epsilon(z) = \begin{cases} n_c^2, & \text{if } z \geq h \\ n_f^2, & \text{if } 0 < z < h \\ n_s^2, & \text{if } z \leq 0 \end{cases} \tag{1.2.6}$$

Substituing the relative dielectric constant on the Maxwell's equation we get three sets of Maxwell's equation with a constant dielectric constant:

$$\nabla \cdot \mathbf{E}_j(\mathbf{r},\omega) = 0 \tag{1.2.7}$$
$$\nabla \times \mathbf{E}_j(\mathbf{r},\omega) = i\omega\mu_0 \mathbf{H}_j(\mathbf{r},\omega) \tag{1.2.8}$$
$$\nabla \cdot \mu_0\mathbf{H}_j(\mathbf{r},\omega) = 0 \tag{1.2.9}$$
$$\nabla \times \mathbf{H}_j(\mathbf{r},\omega) = -i\omega n_j^2 \epsilon_0 \mathbf{E}_j(\mathbf{r},\omega) \tag{1.2.10}$$

where j can be either c, f or s depending on z as in 1.2.6. We can use the above equation to derive the non-coupled wave equation

$$\begin{aligned} \nabla^2\mathbf{E}_j(\mathbf{r},\omega) - k^2 n_j^2 \mathbf{E}_j(\mathbf{r},\omega) &= 0 \\ \nabla^2\mathbf{B}_j(\mathbf{r},\omega) - k^2 n_j^2 \mathbf{B}_j(\mathbf{r},\omega) &= 0 \end{aligned}$$

$$\begin{aligned} \nabla^2\mathbf{E}_j(\mathbf{r},\omega) - k^2 n_j^2 \mathbf{E}_j(\mathbf{r},\omega) = 0 \\ \nabla^2\mathbf{B}_j(\mathbf{r},\omega) - k^2 n_j^2 \mathbf{B}_j(\mathbf{r},\omega) = 0 \end{aligned}, \text{ for } j = c, f, s$$

where $k = \frac{\omega}{\sqrt{\epsilon_0\mu_0}}$. The Ansatz to the equation is a plane wave.
Using the plane wave as the ansatz
Where standard plane wave ansatz can be used

$$\psi_j = A_j \exp\left[\boldsymbol{\beta}\cdot\mathbf{R} + \kappa_j z\right]$$

where $\boldsymbol{\beta} = \beta_x\hat{x} + \beta_y\hat{y}$, $\mathbf{R} = x\hat{x} + y\hat{y}$ and

$$\beta^2 + \kappa_j^2 = n_j^2 k^2$$

where $\beta = |\boldsymbol{\beta}|$

Boundary conditions couples a set of Maxwell equations, and therefore its solutions, from one region to its neighboring region as follows:

$$\begin{aligned} \hat{z} \cdot \left(n_k^2 \mathbf{E}_k - n_j^2 \mathbf{E}_j \right) &= 0, \\ \hat{z} \cdot (\mathbf{B}_k - \mathbf{B}_j) &= 0, \\ \hat{z} \times (\mathbf{E}_k - \mathbf{E}_j) &= 0, \\ \hat{z} \times (\mathbf{H}_k - \mathbf{H}_j) &= 0, \end{aligned}$$

where k, j are either c, f or f, s and $\hat{z}$ is the unitary vector normal to the interface between different materials. Applying the boundary conditions, two sets solutions arise. Each set is characterised by the abscence of the transversal component of either electric or magnetic field. The solution which has no normal component of the magnetic field is called TM and the solutions which the normal component of the electric field are absent are called TE.

, the conditions arises

$$\tan h d_f = \frac{d_f \left(d_c + d_s \right)}{h^2 - d_c d_s}$$

$$d_j^2 = \beta^2 - k^2 n_j^2$$

1.3 Dispersion in Silicon

1.4 Rectangular waveguide

1.4.1 fem

TE-TM

1.5 Bending radius

1.6 Ring resonators

simple - add-drop - eficiency

1.7 Coupling light to the chip

1.8 Active components

1.8.1 Thermo optic effect

1.8.2 Eletrooptic effect

1.8.3 Plasma dispersion

1.9 Light sources

1.10 Detectors

1.11 Fabrication Tecniques

Chapter 2

Spectrometers

2.1 Introduction to spectrometer

2.1.1 Grating equation

2.1.2 Resolving power

Cramming more in less

As shown in section 2.1.2 the necessary grating size required for achieve a given spectral resolution grows with the reciprocal of its size. However this estimation does not include the area needed to transport the light to and from the grating. Indeed, the one stigmantic point correction sugest that the area used plays a key role in the process of spatialy discrimination of spectrum.

K space to position space.

Equation X shows how frequency domain is mapped into K space. however an additional device is needed in order to transform from K space to position space. But a further inspection of the frequency to K domain transformation shows that there is no reason why the transformation cannot be done to position space directly.

2.2 Spectrometer mountings

from angle to point

2.2.1 Czerny-Turner

2.2.2 Rowland

2.2.3 AWG

2.3 Size

2.4 Aberrations

2.4.1 One point stigmatic correction

2.4.2 Two points stigmatic correction

2.5 Blazing and Groove size

2.6 Rayleigh-Huygens model

Chapter 3

Ring enhanced spectrometer

How can we use resonators to make spectrometer. An array of resonators can be used. But fabrication limits prevent its use without requiring individually tunning each resonator. Grating spectrometers uses a lot of space. Is there a middle way. Yes! we can use small free spectral range resonators and a grating spectrometer. The device described in this chapter was published on optics express and presented on the Conference of Lasers and Electro-Optics 2010 (CLEO) as a invited paper and received and honorable mention in the Maiman Student Paper Competition.

3.1 Device Theory

The principle of operation consists of using a resonator to pre-filter the light to be analized by a diffraction grating spectrometer as shown in figure 3.1.1. The resonator transmits only the resonant wavelengths. A diffraction grating spectrometer is then used to route light from different resonances into distinct output channels. The net effect is that the final resonator and diffraction grating spectrometer linewidth will be equal to the resonator linewidth. On silicon ring resonatores cladded with silicon dioxide, linewidth as narrow as 30 pm are rountinely achieved[ref]. Therefore, enabling the possibility of creating 30 pm resolution spectrometers.

To achieve this, the resonator and the spectrometer must be designed so that the channel spacing of the diffraction grating spetrometer matches the ring resonator FSR.

The spectrometer must be designed so that each output channel only allows to transmit a single resonance. Therefore the spectrometer channel spacing must be equal to the resonator FSR.

The spectral resolution of the composed resonator and spectrometer can be estimated as follows.

The transmission spectrum of the composed resonator and spectrometer is the product of the resonator and spectrometer transmission spectrum, as shown in figure 3.1.2.a.

In the described configuration

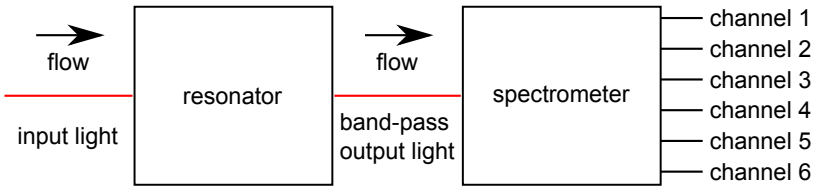

Figure 3.1.1:

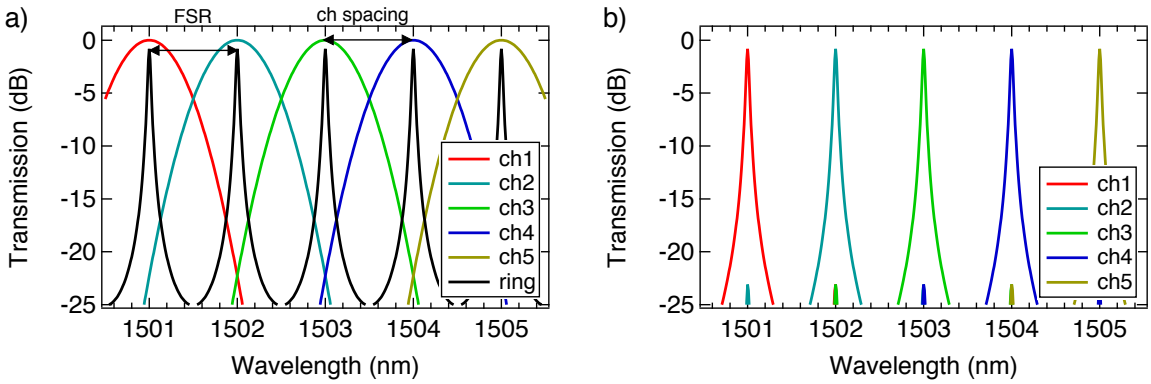

Figure 3.1.2:

3.2 Design

We design the DG spectrometer using the Rowland architecture. To reduce spherical aberration, a non-uniform groove spacing is employed [20]. Metal heaters are added above the silicon layer [21] to align the resonator and spectrometer transmission combs using the thermo-optic effect in silicon. The diffraction grating spectrometer contains 25 channels with spacing of 1 nm. To match the ring resonator FSR to the DG spectrometer channel spacing we use an 83.5 m radius ring with waveguide cross-section of 450 x 250 nm. The FSR changes with wavelength according to $2\lambda/(n_g L)$, but considering a slight positive group velocity dispersion ($\partial n_g/\partial\lambda \approx 3.6 \times 10^{-3}\text{nm}^{-1}$) this change is extremely small: the total change in FSR across the range of operation (25 nm) is approximately 1% for light polarized in the plane of the device (TE polarization).

3.3 Fabrication

The fabrication was done in the Cornell Nanoscale Facility (CNF), http://www.cnf.cornell.edu. A research microfabrication laboratory, funded in part by the National Science Foundation (NSF) and by its users. The research facility counts with state of the art electron beam lithography writer.

We fabricate the device using a CMOS compatible process. We start with a silicon-on- insulator

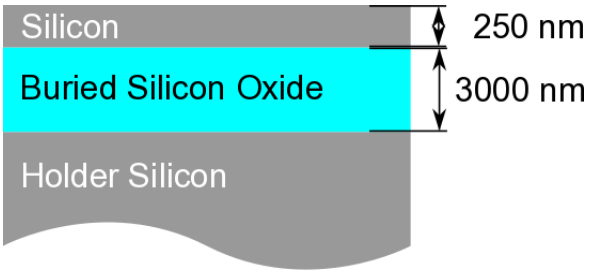

Figure 3.3.1:

(SOI), manufactured by Soitec (http://www.soitec.com) wafer with a 250 nm top silicon layer and a 3 μm buried oxide layer. A 60 nm layer of SiO_2 is deposited using high-temperature low-pressure chemical vapor deposition (HTO) to be used as a hard mask. The grating, ring and waveguides are defined by e-beam lithography on a PMMA resist mask. The pattern is transferred to the oxide layer using a CHF_3/O_2 reactive ion etch (RIE). The silicon layer is etched using chlorine RIE. A layer of 160 nm of SiO_2 is deposited using HTO to conformally fill the 100 nm gaps in the waveguide to ring coupling, then 1 μm of SiO_2 is deposited using plasma enhanced chemical vapor deposition to clad the device. We define the heaters using photolithography (using SPR955CM and LOR5A resists) and then deposit a NiCr film. After liftoff, the wafer is diced and polished for optical testing.

3.4 Testing

We measure the device transmission spectrum by coupling laser light from a tunable laser into the input waveguide using a lensed fiber and measuring the transmitted power as a function of wavelength. The input light is TE polarized and the output light is collected using a microscope objective and filtered for the TE polarization before detection. We achieve a channel FWHM of 0.05 nm across 10 different channels of the composed ring and EDG spectrometer, which represents a decrease in the channel width by 10 times compared with the DG spectrometer alone. This channel width corresponds to a quality factor of Q = $\lambda/\Delta\lambda$= 30000.

Figure 3(b) shows the device transmission. The transmission is normalized to the ring through port power level to eliminate coupling losses. The device insertion loss varies between -18 and -23 dB, where -10 dB is due to the Fresnel reflection of the diffraction grating and can be eliminated by coating it with a metal or using Bragg reflectors [9]. Other losses are attributed to stitching in the waveguide definition during e-beam lithography. A small mismatch between the resonator FSR (0.97 nm) and the DG spectrometer channel spacing (1 nm) cause a misalignment between the resonance and the DG spectrometer channel that builds up from one channel to the next in a Vernier effect. The outcome is a misalignment between the 11th spectrometer channel and the

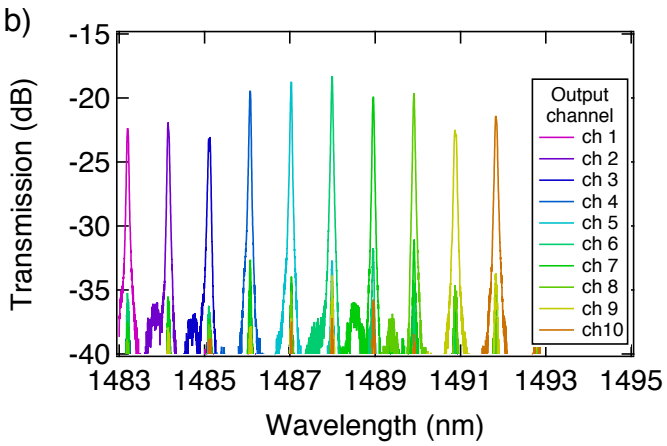

Figure 3.4.1:

11th ring resonance. Therefore only 10 of the 25 channels on the DG spectrometer are used. This issue can be eliminated by more detailed characterization of fabrication.

3.5 Increasing Channel Density

Serializing devices either spatially or in time can increase the spectrometer channel density. The space serialization approach consists of using multiple combined ring-DG spectrometers, so that the input of a spectrometer is connected to the through port of the previous device, as shown in Fig. 4(a). The peak wavelength of each spectrometer is shifted relative to the others. The number of devices needed in order to achieve the a spectral density where the channels are separated by $\Delta\lambda_{FWHM}$, is equal to the DG spectrometer channel width divided by $\Delta\lambda_{FWHM}$. In spite of the area increase, this approach is still more compact than using a traditional diffraction grating spectrometer since in this proposed approach the area increases linearly with resolution as opposed to quadratic in traditional DGs.

In time serialization, Fig. 4(b), only a single combined spectrometer is used and the output spectrum is measured several times. In each measurement the device transmission spectrum is shifted. Notice that this approach also requires active tuning of the ring and the EDG spectrometer. By applying the time serialization technique we were able to reduce the channel spacing from 0.97 nm to 0.097 nm, and were able to measure 100 channels using the device.

A zoom in on the series of channels is depicted in Fig. 6 (a). Figure 6 (b) shows a density plot where each horizontal line corresponds to the transmission spectrum of each channel. Notice that the overlap of the residual transmission from the DG spectrometer with the neighboring resonances can be seen in the side diagonal lines, and their transmissions are at least 10 dB lower than the peak (main diagonal line).

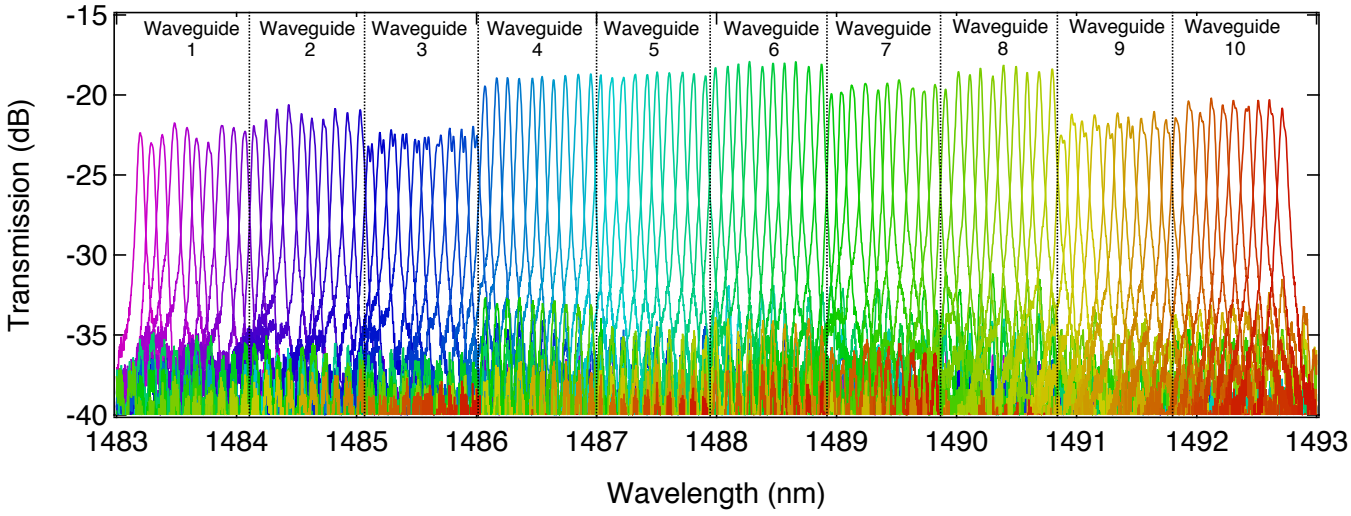

Figure 3.5.1:

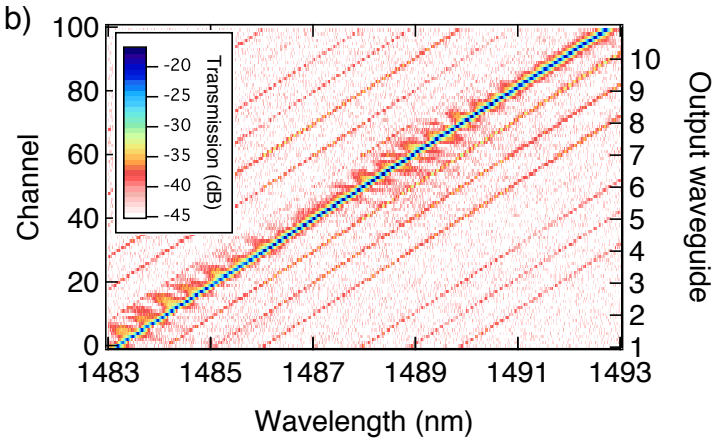

Figure 3.5.2:

Cross talk from neighbohring channels

adsfasdf

dfsdfasd

3.6 Effect of transmission spectrum lineshape